DALAT UNIVERSITY JOURNAL OF SCIENCE Volume 11, Issue 4, 2021 98-112

THE EFFECT OF CRITICAL ELECTRIC FIELDS ON THE ELECTRONIC DISTRIBUTION OF BILAYER ARMCHAIR GRAPHENE NANORIBBONS

Nguyen Lam Thuy Duong[a], Nguyen Thi Kim Quyen[a, b], Pham Nguyen Huu Hanh[a], Le Dang Khoa[c], Ngo Van Chinh[d], Phan Thi Kim Loan[c], Huynh Anh Huy[c], Vu Thanh Tra[c*]

[a]School of Graduate, Can Tho University, Can Tho, Vietnam
[b]The Faculty of Engineering-Technology, Kien Giang University, Kien Giang, Vietnam
[c]Department of Physics, School of Education, Can Tho University, Can Tho, Vietnam
[d]Ho Thi Ky High School, Ca Mau, Vietnam
[*]Corresponding author: Email: vttra@ctu.edu.vn

Article history
Received: September 27th, 2021
Received in revised form: October 26th, 2021 | Accepted: November 8th, 2021
Available online: December 6th, 2021

Abstract

We employed tight-binding calculations and Green's function formalism to investigate the effect of applied electric fields on the energy band and electronic properties of bilayer armchair graphene nanoribbons (BL-AGNRs). The results show that the perpendicular electric field has a strong impact on modifying and controlling the bandgap of BL-AGNRs. At the critical values of this electric field, distortions of energy dispersion in subbands and the formation of new electronic excitation channels occur strongly. These originate from low-lying energies near the Fermi level and move away from the zero-point with the increment of the electric field. Phase transitions and structural changes clearly happen in these materials. The influence of the parallel electric field is less important in changing the gap size, resulting in the absence of the critical voltage over a very wide range [–1.5 V; 1.5 V] for the semiconductor-insulator group. Nevertheless, it is interesting to note the powerful role of the parallel electric field in modifying the energy band and electronic distribution at each energy level. These results contribute to an overall picture of the physics model and electronic structure of BL-AGNRs under stimuli, which can be a pathway to real applications in the future, particularly for electronic devices.

Keywords: Bilayer armchair graphene nanoribbons; Electronic band structures; Parallel electric field; Perpendicular electric field.

DOI: http://dx.doi.org/10.37569/DalatUniversity.11.4.973(2021)

Article type: (peer-reviewed) Full-length research article

1. INTRODUCTION

Graphene is presently the subject of much research focused on mass manufacturing, characterization, and potential applications. This material is drawing considerable attention among research groups worldwide due to its distinctive electronic features (Novoselov et al., 2012; Scholz et al., 2012; Abergel et al., 2010; Dubois et al., 2009; Neto et al., 2009) and structural diversity (Zhong et al., 2012; Ruseckas et al., 2011). With both monolayer and bilayer states (including AA- and AB-stacking patterns) and diverse structural forms, graphene exhibits intriguing physical properties. Examples include the interlayer interaction that reshapes the linear dispersion in monolayer graphene into the parabolic dispersion in double-layer graphene (Li et al., 2009; Abergel & Fal'ko, 2007) and the ability of the interlayer interaction to tailor the metallic or semiconducting state efficiently by using different stimuli (Castro et al., 2007; Bai et al., 2010; Loan et al., 2014).

In particular, due to its structural stability and outstanding physical behavior (Zhong et al., 2012; Xu et al., 2009; McCann & Koshino, 2013), bilayer graphene nanoribbons have been the subject of numerous theoretical and experimental studies (Zhong et al., 2012; Malard et al., 2008; Nanda & Satpathy, 2009). Many of these studies focus on the conductivity and properties of this material in the presence of external influences (Castro et al., 2007; Bai et al., 2010; Ohta et al., 2006) for use in electronic device applications. It is noteworthy that the external electric fields, including the perpendicular and parallel electric fields, are among the stimuli that have received the most attention from the scientific community (McCann, 2006; Min et al., 2007; Zhang et al., 2009; Mak et al., 2009). Previous studies have shown that in the BL-AGNR structure, the perpendicular electric field has a significant impact on tuning the bandgap of the material. On the other hand, the parallel electric field has a greater influence on the energy dispersion of zigzag bilayer graphene (Vũ & Trần, 2016; Vũ et al., 2017). Similar analytical calculations for each dimer line corresponding to each termination state have demonstrated that the maximum magnitudes of the gap are dissimilar for different critical potential strengths (Vũ & Trần, 2016; Vũ et al., 2017; Vũ et al., 2018). In particular, the gap size for the armchair edge is E_{gap_max} = 400 meV under the effect of $|V_t| = 0.96$ V for M = 16 or E_{gap_max} = 350 meV with $|V_t| = 1.3$ V for M = 17 (Vũ et al., 2017). For the zigzag edge, the energy gaps of $M = 16$ and $M = 19$ have peaks of approximately 450 meV and 369 meV at $|V_s| = 1.14$ V and $|V_s| = 0.92$ V, respectively (Vũ & Trần, 2016).

However, extensive investigations of the consequence of each type of electric field on the charge distribution and electronic band structure of the material are few. The phenomena occurring in the electronic structure at critical or overcritical electric fields, in particular, are still a mystery and require a proper explanation. Therefore, our research aims to provide a comprehensive understanding of the influence of external electric fields on BL-AGNRs and to demonstrate how the charge-carrier redistribution affects the energy dispersion of this material at critical voltages and voltages higher than critical. Such understanding is necessary for constructing a foundation for suitably using such materials in the semiconductor-transistor industry. Our paper examines the following

topics: (1) the modification of energy band structures for BL-AGNRs under the impact of external electric fields, (2) the manipulation of material conductivity over a certain range of external fields, and (3) the effect of critical and overcritical voltages on the electronic structure of the material.

2. MODELING AND METHODOLOGY

2.1. Modeling

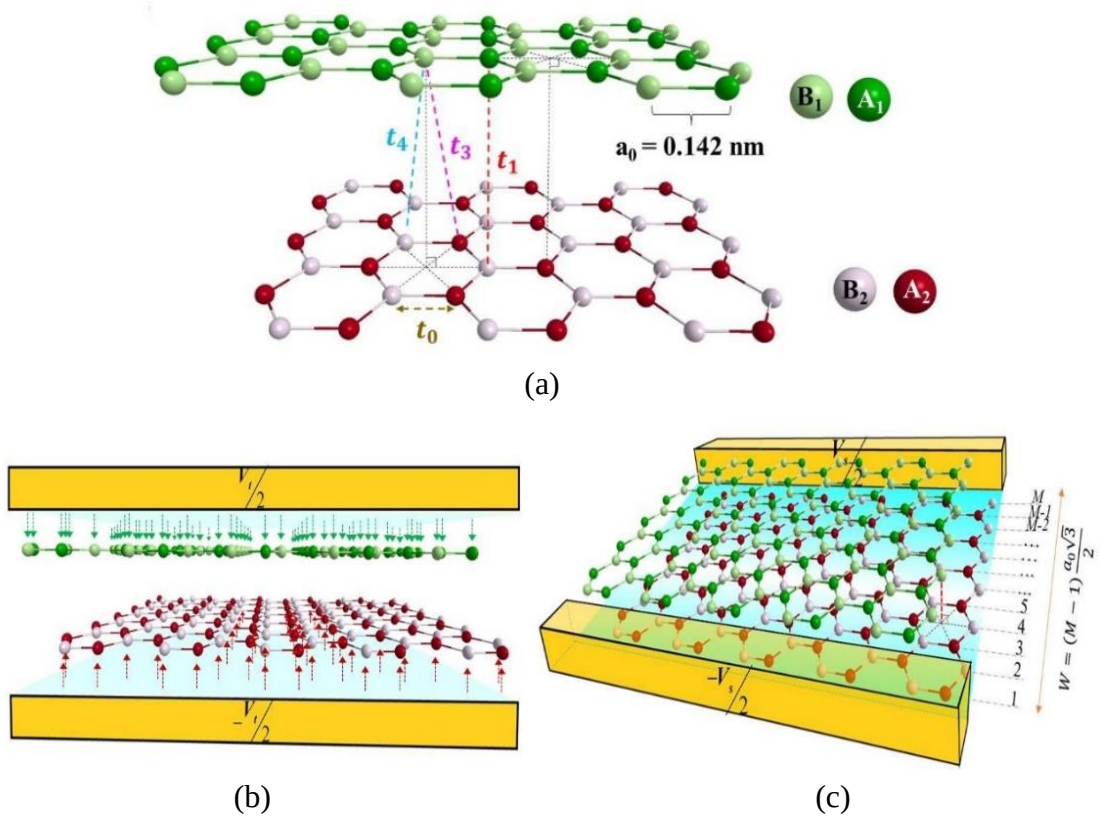

(a)

(b) (c)

Figure 1. Schematic of BL-AGNRs: (a) AB-stacking model and the effects of (b) perpendicular and (c) parallel electric fields

In this paper, we investigated the armchair edge of Bernal-stacked bilayer graphene. To conduct the calculations, we distinguished the positions of the carbon atoms in each layer. In the upper layer, the atoms shown as dark and light green spheres are designated A_1 and B_1, respectively. In the lower layer, the atoms shown as dark and light red spheres are designated A_2 and B_2, respectively. Hence, in the AB-stacking model, the atomic pairs A_1-A_2 and B_1-B_2 have the same characteristics in both layers. It is clear and well known that the structural and electronic properties have a close relationship. Usually, an appropriate structure is determined by its physical properties. In this study, using the tight-binding method, the energy band of this material was calculated based on the closest interactions, denoted t_0, and interactions t_1, t_3, and t_4 (shown in Figure 1a) to identify their electronic and structural properties. Parameter t_0 is the hopping energy between the two

nearest atoms in the same layer (A_1-B_1 or A_2-B_2). The other parameters correspond to interlayer interactions. Parameter t_1 is the hopping energy for perpendicular atoms (A_1-B_2), and t_3 is the hopping energy for non-perpendicular (B_1-A_2) atoms. Parameter t_4 is the interaction energy between atoms of the same type belonging to two layers (A_1-A_2 or B_1-B_2) (Charlier et al., 1991).

Earlier studies (Castro et al., 2007; Vũ & Trần, 2016; Vũ et al., 2017; Vũ et al., 2018) have revealed intriguing results on the controllable energy gap of this material by utilizing perpendicular and parallel electric fields. Thus, to examine the arrangement of electrons or the charge distribution under the impact of stimuli (specifically at the critical values of the electric fields), models are constructed that express the effect of each field on BL-AGNRs, as shown in Figure 1b-c. In particular, we assume in these models that the effects of the perpendicular and parallel gates are substantial enough to directly affect each atom without changing the material's geometric structure. The perpendicular electric field is generated by two gates (shown as yellow in Figure 1b) in the upper and lower BL-AGNR layers corresponding to field strengths, $\frac{V_t}{2}$ and $-\frac{V_t}{2}$. In Figure 1c, two side gates, $\frac{V_s}{2}$ and $-\frac{V_s}{2}$, are generated along with the armchair edges of the BL-AGNRs, leading to the creation of the parallel electric field. The width W between the two edges of the BL-AGNRs is $W = (M-1)\frac{a_0\sqrt{3}}{2}$, where $a_0 = 0.142$ nm is the distance between the two nearest carbon atoms, and M represents the number of dimer lines along the ribbon width. By combining this model with the Green's function formalism and the tight-binding method, we calculate and investigate the adjustment of the electronic distribution when the external fields are applied.

2.2. Methodology

To find a solution for the band structure, we use the Schrodinger equation as presented in Formula (1). In which, H is the Hamiltonian operator, with the eigenvalue E and Ψ_0 is the wave function.

$$H\psi_0 = E\psi_0 \tag{1}$$

and to investigate the electronic distribution under the impact of external electric fields, we build a computational model, expressed as Equation (2), based on the tight-binding method (Cresti et al., 2008):

$$H = \sum_i \varepsilon_i |i\rangle\langle i| + \sum_{\langle ij\rangle} t_{ij}\left(|i\rangle\langle j| + |j\rangle\langle i|\right) + \sum_i U_i |i\rangle\langle i|. \tag{2}$$

The first and second terms in Equation (2) represent the intrinsic energies of the BL-AGNRs, and the third term represents the newly added energy. Specifically,

- ε_i: Onsite energy of carbon atoms set to $\varepsilon_i = 0$ (Cresti et al., 2008) for the convenience of the calculations.

- t_{ij}: Interaction energies of carbon atoms in the same layer and between two layers, as shown in Figure 1a. The parameters $\{t_0, t_1, t_3, t_4\}$ are taken from *ab initio* calculation results (Son et al., 2006; Sun & Chang, 2008) corresponding to values $\{2.598\,eV, 0.364\,eV, 0.319\,eV, 0.177\,eV\}$.

- U_i: Energy added at the i^{th} site. Here, we use the individual perpendicular and parallel electric fields as the external stimuli acting on the material's structure. Hence, U_i will be expressed as follows:

  (i) For the perpendicular electric field, $U_i = \pm e\frac{V_t}{2}$, energy is added for each atom in the upper (+) and lower (–) layers of the BL-AGNRs, as shown in Figure 1b.

  (ii) For the parallel electric field, $U_i = -e\left(-\frac{V_s}{2} + E_{//} d_i\right)$ with $E_{//} = \frac{V_s}{W}$ and d_i as the distance from the i^{th} atom to the initial gate (with the original electrode chosen as $-\frac{V_s}{2}$), as presented in Figure 1c.

In addition, to clarify the contribution of the electrons in the energy spectrum, we compute the density of states (DOS) based on Equation (3) (Datta, 2005):

$$DOS(E) = \frac{i \times trace\left[G(E) - G(E)^{+}\right]}{2\pi}, \tag{3}$$

where $G(E)$ is expressed explicitly according to the Green's function method (Datta, 2005):

$$G(E) = \left[\left(E + i0^{+}\right)I - H\right]^{-1}. \tag{4}$$

3. RESULTS AND DISCUSSION

3.1. The electronic structure of BL-AGNRs under the effect of external electric fields

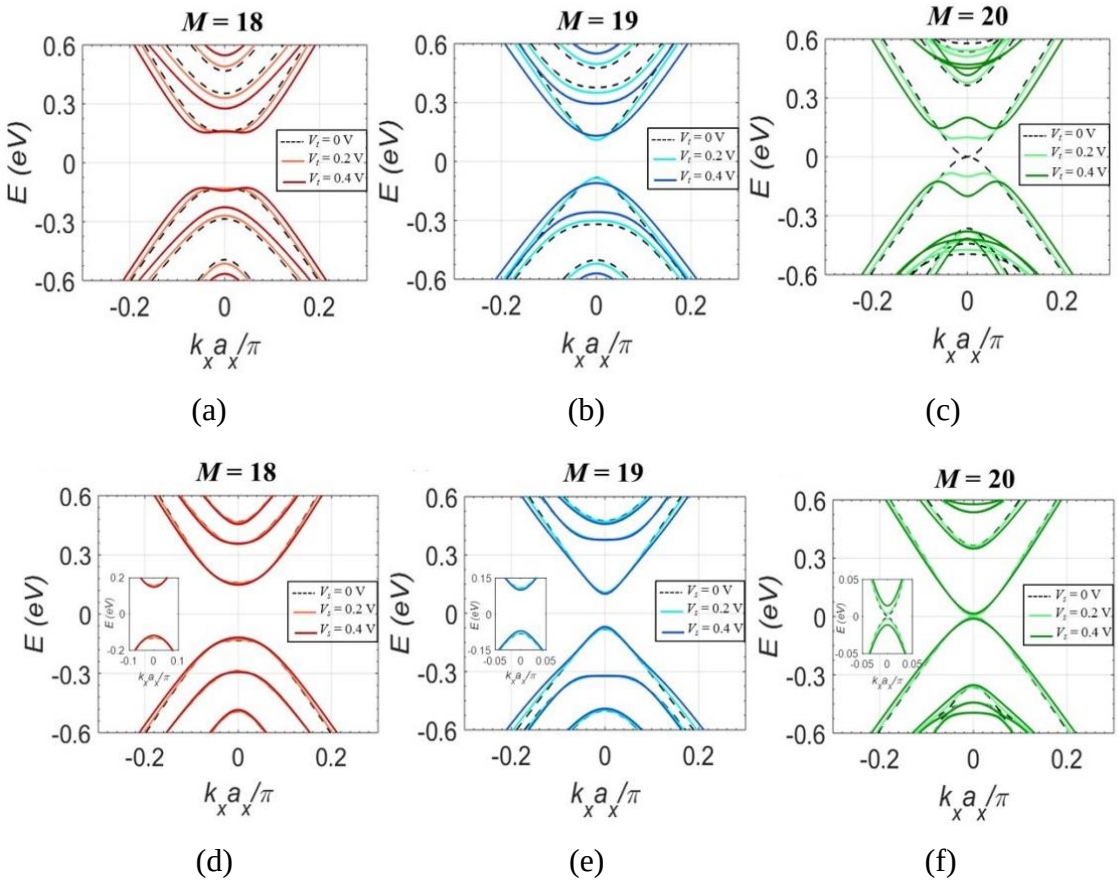

Figure 2. Effect of the external (a-c) perpendicular electric field and (d-f) parallel electric field on the gap size in BL-AGNRs with dimer lines (*M* = 18, 19, 20)

Figure 2 shows changes in the gap size of the band structure of BL-AGNRs with and without perpendicular and parallel external electric fields. From the results illustrated in Figure 2, it is very clear that the different values of the applied electric fields affect the three groups, $M = 3p$, $3p + 1$, and $3p + 2$, differently as represented by each dimer line M = 18, 19, and 20 (where p is a positive integer). Following previous studies (Vũ et al., 2017; Khaliji et al., 2013), the sequence of dimer lines in the range [3; 20] effectively enhances the bandgap. With the applied external fields, three ribbon widths, M = 18, 19, and 20, will cause the enhancement because of their ability to cause a transition of the material properties from the insulator to the metal state. Under the impact of the perpendicular electric field, the bandgaps of dimer lines in the semiconductor group (represented by M = 18 and M = 19) decrease with an increase in applied voltage, i.e., 0 V, 0.2 V, and 0.4 V, as seen in Figure 2a-b. However, the results for M = 18 differ from those for M = 19; i.e., the electronic structure is altered more clearly when the electric

field, $V_t = 0.4$ V is applied. Two parabolic peaks are created instead of one initial peak, as represented by dark pink in Figure 2a. The modifications in the bandgap and the band structure for $M = 18$ are stronger than those for $M = 19$. It is shown that the transition to the metallic state for $M = 18$ is faster than for $M = 19$. More interestingly, in Figure 2c, the results obtained for $M = 20$ are the opposite of those in the previous two cases. The original state of this material is metallic with zero gaps, and when the applied perpendicular electric field is increased from 0.2 V to 0.4 V, the bandgap opens effectively with a value depending on the magnitude of the applied potential strength. Simultaneously, its band structure also clearly changes with the electric field. These results reveal the rearrangement of electrons in the excited energy levels under the influence of the parallel electric field. For group $3p + 2$, represented by $M = 20$, the metal-semiconductor transition occurs under the influence of the external field. The result strongly suggests that the perpendicular electric field plays a major role in controlling the conductivity of this group.

In Figure 2d-f, we examine the effect of the parallel electric field in BL-AGNRs with voltages of the same magnitude as the perpendicular fields. Our results (shown in the inset figures) reveal that the energy levels in the band structure remain unchanged compared to those without an applied electric field. Nonetheless, when comparing the influence of the perpendicular field among the three groups, the case of $M = 20$ (Figure 2f) shows the strongest effect in modulating the band structure. These results are similar to those for the perpendicular fields.

Based on the above investigations, we concluded that when employing the same voltages, the parallel electric field is less dominant than the perpendicular field in controlling the bandgap and tuning the electronic structure. There are two possible explanations for this disparity. Firstly, in the case of the perpendicular electric field, the electric potential V_t will be added directly to each atom and generated from the top to the bottom layer, and inversely (Figure 1b), independent of the ribbon width. The electric gates, $\frac{V_s}{2}$ and $-\frac{V_s}{2}$, which induce the parallel fields, are set to the upper and lower edges of the ribbon simultaneously or applied from outbound to inner lines of the graphene nanoribbons (Figure 1c), which means that a number of atoms received the electric fields and generated effectively. Thus, the influence of the parallel electric field will depend explicitly on the number of dimer lines, M. Secondly, previous research studies (Vũ et al., 2017; Sahu et al., 2010; Lam & Liang, 2008) have shown that the larger the ribbon for BL-AGNRs, the narrower the bandgap. Importantly, in the region of $M \geq 20$, the bandgaps of all three groups tend to zero, leading to metallic behavior for the infinite graphene sheet. Therefore, it is a difficult task to control the gap of dimer lines ($M = 18, 19, 20$) with only small values of V_s. Thus, to change the gap or the conductivity of this material, it is necessary to enhance the role of electrostatic fields or strengthen the bias voltages. However, does it have any limitation on the field intensity? Furthermore, what are the requirements to attain the best efficiency in changing the gap size without disrupting the electronic structure? To answer these questions and to understand the impact of the fields more thoroughly, and at the same time, to identify the values of the

required field for each dimer line, M, we further examine the energy gap as a function of $V_t(V_s)$ in Figure 3.

3.2. The effect of external electric fields on the bandgap of the material

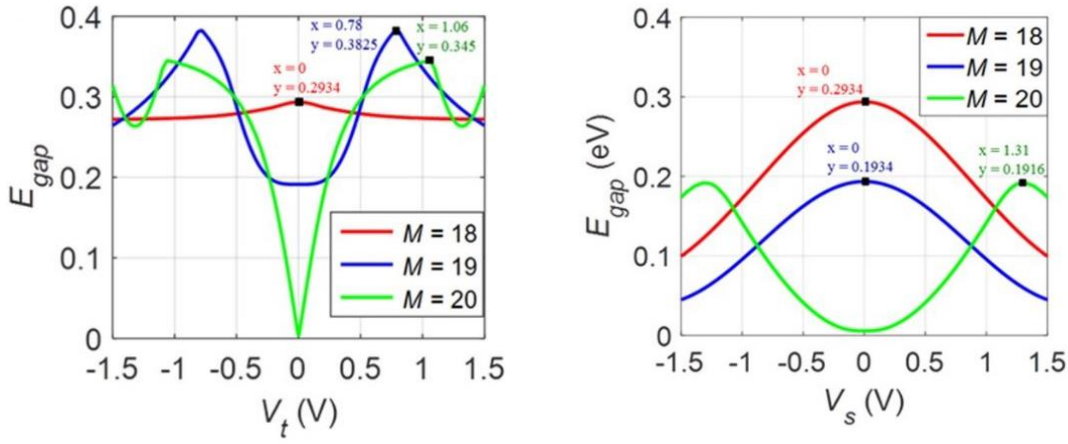

(a) (b)

Figure 3. Dependence of the bandgaps on the external (a) perpendicular electric field and (b) parallel electric field, where *x* is the magnitude of the electric field and *y* is the gap size

To find the rules for the modulations in the band structure and the distribution of electrons, and to determine the critical states of the material under the effect of the external fields, we investigated the role of the electric fields in the interval V = [–1.5 V; 1.5 V].

Figure 3a provides an opportunity for us to summarize the overall picture and discuss the detailed physics. The impact of the perpendicular electric field and the alteration of the bandgap of three separate structural groups may follow two rules. Firstly, the bandgap does not appear to vary and only falls into a small, narrow gap for the 3p group, represented by M = 18 (the red line). Secondly, the bandgap widths vary dramatically for the two other groups, 3p + 1 and 3p + 2, corresponding to M = 19 (the blue line) and M = 20 (the green line), respectively. In particular, the intrinsic bandgaps of M = 19 and M = 20 without electric fields are 190.6 meV and 0 meV, respectively. After that, when we apply the voltages V_t with gradual increments in the range [0; 0.78 V] for M = 19 and [0 V; 1.06 V] for M = 20, the BL-AGNR bandgaps demonstrate an upward trend. If the potential values continue to rise beyond the above range, the bandgaps decrease for both structures. Thus, before the reversal phenomenon of phase transition, the bandgap is reduced. These gap values will reach peaks at E_{gap_max} = 382.5 meV and E_{gap_max} = 345 meV, respectively, at the critical values $|V_t|$ = 0.78 V for M = 19 and $|V_t|$ = 1.06 V and for M = 20. At the same time, the findings also strongly demonstrate that the gap modifications in dimer line M = 20 are stronger than those in M = 19 despite $E_{gap\_max\,(M\,=\,20)} < E_{gap\_max\,(M\,=\,19)}$. For these reasons, the results confirm that the perpendicular electric field has a significant effect in expanding the bandgap of the metal group (represented by M = 20) in the BL-AGNRs. Moreover, it is worth noting that the M = 19

dimer line is characterized for the semiconductor-dielectric group. However, under the existence of the perpendicular electric field, the tunability in the bandgap for $M = 19$ is similar to that for $M = 20$. These results demonstrate the intriguing effects of a perpendicular electric field in controlling the bandgap of a material with such specific dimer lines.

In addition, from observations of the modulations of the bandgap in the range $V_t = [-1.5\text{ V}; 1.5\text{ V}]$, we found that for all three dimer lines, the bandgaps open (or narrow) symmetrically according to the symmetrical values of V_t. The cause of this behavior is that the perpendicular electric field originates from the electrodes and goes farther to each layer (upper/lower layer) of the BL-AGNR sheet. Therefore, the electric fields provide atoms in the upper and lower layers with the energies $e\frac{V_t}{2}$ and $-e\frac{V_t}{2}$, respectively. When we change the position of the electrodes or alter/reverse the direction of the electric fields acting on the atoms in the upper and lower layers, the corresponding electric energies are $-e\frac{V_t}{2}$ and $e\frac{V_t}{2}$ for each layer, respectively. Thus, due to the periodic structure in our Hamiltonian model, when the perpendicular external field is applied, the intensity of the electric field in the above two cases will have the same effect in modifying and controlling the bandgap of the material when the direction of the electric field is reversed. This allows the bandgap to be tuned symmetrically to the $|V_t|$ values.

On the other hand, to show the effects of the parallel electric field on the conductivity of this material, we examined the bandgap of BL-AGNRs as a function of V_s with different dimer lines, M. The results show that the behavior of the parallel field is the same as that of the perpendicular field for the dimer line $M = 20$ (the blue line in Figure 3). Specifically, under the existence of V_s, the bandgap will reach its highest point, $E_{gap\_max} = 191.6$ meV, and then gradually decrease if the magnitude of the voltage exceeds the critical value, $|V_s| = 1.31$ V. However, with $M = 18$ and $M = 19$ representing the semiconductor-dielectric groups, the bandgaps drop with the increase in the potential values. In particular for $M = 18$, the bandgaps are 293.4 meV, 253.3 meV, and 169.9 meV for the applied V_s values of 0 V, 0.5 V, and 1.0 V, respectively. Likewise, for $M = 19$ and for the same V_s values, the bandgaps are 190.6 meV, 158.7 meV, and 90.3 meV. These results indicate that, unlike the perpendicular electric field, the parallel field will stimulate the transition of semiconductor-dielectric groups more quickly toward the metal properties of this material. However, we strongly confirm that the effective electric fields used to control the energy gap or its properties must be equal to or lower than the critical values because overcritical points of the electric fields may deform the structure.

Hence, by considering the influence of two types of electric fields on modulating the electronic gaps, we realized that the gap size of the material would be narrowed or expanded depending on the type and magnitude of the applied electric fields. For the $3p$ group (represented by $M = 18$), the effect of the parallel electric field is powerful. In contrast, for the $3p + 2$ group (represented by $M = 20$), the perpendicular electric field has a greater influence. In particular, under the external electric fields, the width of the ribbon

will be provided with critical values belonging to certain potential regions. Thus, to find these critical values and the overcritical ones, and to determine how each type of electric field will affect the energy spectrum and the electronic arrangement, we analyze the results in Figure 4.

3.3. Critical and overcritical voltage effects on the electronic structure of the material

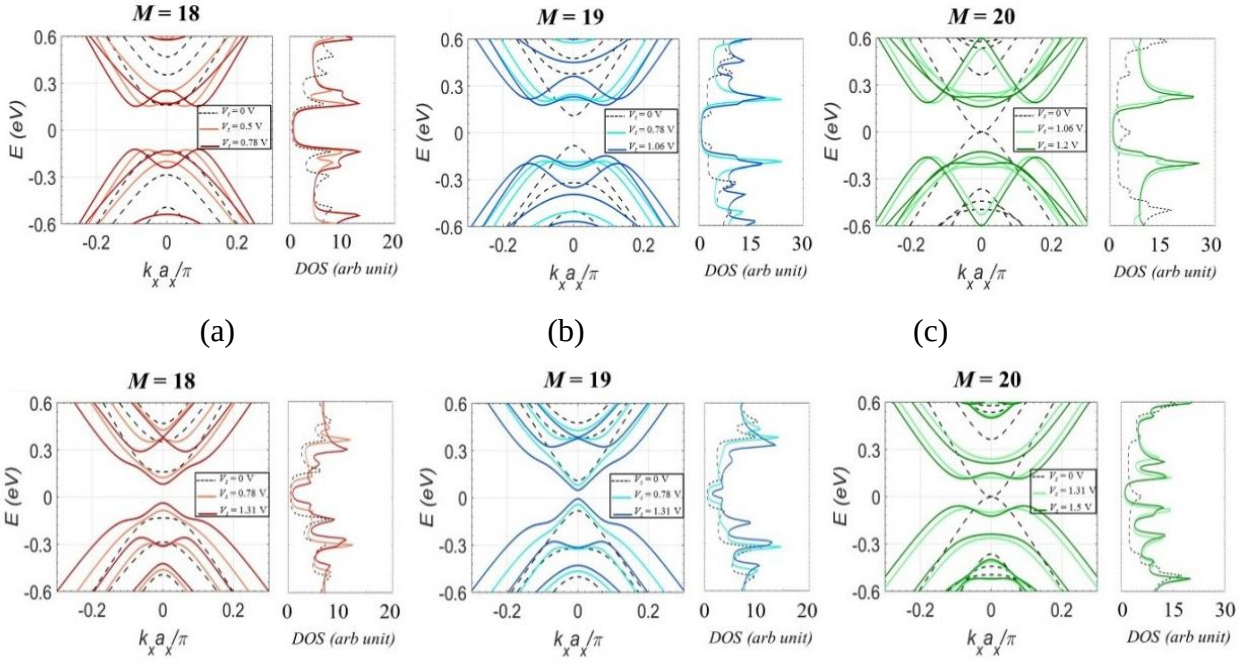

Figure 4. Alteration of energy bands and density of states (DOS) under the effects of critical and overcritical values of (a-c) the perpendicular electric field and (d-f) the parallel electric field

To present a clarified perspective on the modulation of the band structure and the energy shift in the energy dispersion and electronic distribution (DOS) at the critical potential values of V_t and V_s, we discuss the results shown in Figure 4.

First, we inspected the effect of V_t on the electric quantities for all three groups, as in Figure 4a-c. For M = 18, we noted the deformations of subbands in the energy bands with the enlargement of specific field strengths. In particular, when we applied the magnitude of field V_t = 0.5 V, the initial parabolic subbands around the Fermi energy E_F = 0 began to be modified. Moreover, if we set the potential value of the perpendicular field equal to the critical potential strength for M = 19 (V_t = 0.78 V), the electronic structures of the semiconductor-dielectric groups have similar changes, as in Figure 4a-b. Here, in both the valence and conduction bands, the formation of two parabolic subpeaks is symmetrical about the position of k_x = 0. At the same time, the modulations of the peak structure in the DOS (on the right side of the energy band) are also reflected clearly. More

importantly, from the analyses on the effect of the overcritical values in Figure 4b, with V_t = 1.06 V, it can be seen that the appearance of two degenerate energy levels of the valence and conduction bands is located contiguously and symmetrically at the Fermi level. Additionally, based on the observation of the DOS, we found that the position of the splitting peak formed a minor peak adjacent to the principal peak (at nearly the zero points). It demonstrated plainly that the height of these sharp peaks is not prominent as in the case of M = 18. Also, the results in Figure 4c illustrate that the screening effect of the splitting peak for M = 20 is similar to that of M = 19 at two values: the critical value (V_t = 1.06 V) and the overcritical value (V_t = 1.2 V). However, the splitting effect of group 3p + 2 happens vigorously and even plays an important role in the subbands moving far away from E_F = 0. This again confirms the strong ability of the perpendicular electric field to enlarge the gap size at M = 20 for this material.

From these investigations, we realized that by varying the magnitude of the electric field from zero to the critical potential strength (to obtain the maximum value of E_{gap}), the perpendicular field could be used to control the energy gap of this material. However, if the critical potential strengths are exceeded (over the critical values of the electric fields), the electronic structure change is complex, particularly in the metal group, as shown by M = 20 in Figure 4c. To elucidate this phenomenon, we consider the model calculation based on the tight-binding approximation. Therein, the hopping energy employed, t_0 = –2.589 eV, is the nearest interaction. The added external fields play a role in a small perturbation potential to use in the calculation. Therefore, to apply a large field strength (over the critical electric potential), the influence of the electric field can break the bonding order, leading to a modification of the shape of the subbands in the energy band and an electronic redistribution, and it will modify the structure. Simultaneously, as in the analyses, the perpendicular field strongly affects the energy level adjoining the Fermi energy and is far from E_F = 0 for this structure (Vũ et al., 2017; Vũ et al., 2018; Castro et al., 2008). From this, it is predicted that modulations will occur and the structure will be destroyed when the critical V_t is exceeded.

Moreover, in similar investigations at the critical and overcritical values for the same dimer lines under the effect of a parallel electric field, we obtain the intriguing consequences shown in Figure 4d-f. Following the results in Figure 3b for semiconductor-dielectric groups, the limitation of V_s = [–1.5 V; 1.5 V] will not appear at the critical potential strength of E_{gap_max}. Therefore, for a better examination, we employ the voltage values V_s = 0.78 V and 1.31 V in the electric potential range, inducing clear modulations of the gaps that correspond to the critical field region mentioned in applying the V_t effect. The results show that for V_s = 1.31 V applied to the M = 18 and 19 cases, the parabolic subbands are distorted to form sharp peaks at the top of valence bands (n_v) and the bottom of conduction bands (n_c), producing narrower gaps. This phenomenon might lead to electronic mobility in the displacement between these two bands n_c and n_v, resulting in faster semiconductor-insulator-to-metal transitions. Simultaneously, the DOS spectrum indicates the various distributions of the spectral peak, demonstrating that the rearrangement of the electrons was accompanied by increased excitation channels when applying an increment of potential strength (Chang et al., 2006; Lu et al., 2006). More

importantly, when examining the electronic properties of $M = 20$ in the presence of the parallel field, the results showed similarities to those of the perpendicular field. In other words, the expansion of the gap size and the formation of subpeaks in the spectral structure are obvious. Thus, although the values of applied V_s are larger than those of V_t, the impact of the parallel field in causing the splitting effect for BL-AGNRs is not as plain as for the perpendicular field. Nevertheless, the use of V_s at the critical and overcritical values (in certain regions) can serve to control the gap size of this material. This outcome is entirely different from that in the V_t application.

In addition, the above results show that in two groups, $3p$ and $3p + 1$, the arrangement of electrons behaves dissimilarly under the sole effect of each type of electric field. While V_t induces energy degeneracy and peak splitting in the energy and DOS spectra, V_s creates dominant peaks at the bottom of the conduction band and the top of the valence band. However, in the same metal group, $M = 3p + 2$, the effects of V_t and V_s are identical in enlarging the electronic gap and splitting peaks at the critical and overcritical points. We found that with these values, the electric fields have many interesting effects on physical properties, such as altering the gap size, modifying the redistribution of electronic states, modulating the subband shape, and forming diverse spectral peaks. Thus, it can be said that the calculations herein provide a general comparison of the effects of both types of electric fields in modifying the electrical quantities of BL-AGNR structures.

4. CONCLUSIONS

We investigated the influence of perpendicular and parallel external electric fields on the electronic distribution of BL-AGNRs and acquired many fascinating results. At the critical and overcritical values, the effect of each field on the arrangement of electrons differs considerably. In particular, when applying potentials of $|V_t| \geq 0.78$ V for $M = 19$ and $|V_t| \geq 1.06$ V for $M = 20$, the band structure of this material forms degenerate subbands, represented by the existence of two symmetrical parabolic peaks at $k_x = 0$. Simultaneously, the effect of the electric field will increase from the Fermi energy levels to energies far from this point for both the conduction and valence bands. Moreover, similar results can be obtained using the parallel electric field for the metal group ($M = 20$). However, when applying and expanding the potential values in the interval $V_s = [-1.0\text{ V}; 1.5\text{ V}]$ for the semiconductor-insulator groups (represented by $M = 18$ and $M = 19$), the energy gaps narrow and the electrons become more flexible. This is illustrated in the formation of two sharp peaks in linear dispersion, according to the lowest conduction and the highest valence energy levels. In other words, with the potential strengths, $|V_s| \geq 1.0$ V, the arrangement of charge carriers in the energy dispersion of the AB-stacking is changed. Hence, the effect of external electric fields on the electronic band structure of such material depends crucially on the type and intensity of the external fields. At the same time, this study denoted that if we want to tailor the conductivity and obtain maximal values of E_{gap}, the magnitudes of the external electric fields are utilized under the critical values. Moreover, those strongly depend on the number of dimer lines, M.

ACKNOWLEDGMENTS

The Vietnam National Foundation for Science and Technology Development (NAFOSTED) funded this research under grant number 103.01-2018.338.

REFERENCES

Abergel, D. S. L., Apalkov, V., Berashevich, J., Ziegler, K., & Chakraborty, T. (2010). Properties of graphene: A theoretical perspective. *Advances in Physics*, *59*(4), 261-482. https://doi.org/10.1080/00018732.2010.487978

Abergel, D. S. L., & Fal'ko, V. I. (2007). Optical and magneto-optical far-infrared properties of bilayer graphene. *Physical Review B*, *75*, 155430. https://doi.org/10.1103/PhysRevB.75.155430

Bai, J., Zhong, X., Jiang, S., Huang, Y., & Duan, X. (2010). Graphene nanomesh. *Nature Nanotechnology*, *5*(3), 190-194. https://doi.org/10.1038/nnano.2010.8

Castro, E. V., Novoselov, K. S., Morozov, S. V., Peres, N. M. R., Santos, J. M. B. L. D., Nilsson, J., Guinea, F., Geim, A. K., & Neto, A. H. C. (2007). Biased bilayer graphene: Semiconductor with a gap tunable by the electric field effect. *Physical Review Letters*, *99*(21), 216802. https://doi.org/10.1103/PhysRevLett.99.216802

Castro, E. V., Peres, N. M. R., Santos, J. M. B. L. D., Guinea, F., & Neto, A. H. C. (2008). Bilayer graphene: Gap tunability and edge properties. *Journal of Physics: Conference Series*, *129*, 012002. https://doi.org/10.1088/1742-6596/129/1/012002

Chang, C. P., Huang, Y. C., Lu, C. L., Ho, J. H., Li, T. S., & Lin, M. F. (2006). Electronic and optical properties of a nanographite ribbon in an electric field. *Carbon*, *44*(3), 508-515. https://doi.org/10.1016/j.carbon.2005.08.009

Charlier, J. C., Gonze, X., & Michenaud, J. P. (1991). First-principles study of the electronic properties of graphite. *Physical Review B*, *43*(6), 4579-4589. https://doi.org/10.1103/PhysRevB.43.4579

Cresti, A., Grosso, G., & Parravicini, G. P. (2008). Valley-valve effect and even-odd chain parity in p-n graphene junctions. *Physical Review B*, *77*(23), 233402. https://doi.org/10.1103/PhysRevB.77.233402

Datta, S. (2005). *Quantum transport: Atom to transistor*. Cambridge University Press.

Dubois, S. M. M., Zanolli, Z., Declerck, X., & Charlier, J. C. (2009). Electronic properties and quantum transport in graphene-based nanostructures. *The European Physical Journal B*, *72*, 1-24. https://doi.org/10.1140/epjb/e2009-00327-8

Khaliji, K., Noei, M., Tabatabaei, S-M., Pourfath, M., Fathipour, M., & Abdi, Y. (2013). Tunable bandgap in bilayer armchair graphene nanoribbons: Concurrent influence of electric field and uniaxial strain. *IEEE Transactions on Electron Devices*, *60*(8), 2464-2470. https://doi.org/10.1109/TED.2013.2266300

Lam, K. T., & Liang, G. (2008). An *ab initio* study on energy gap of bilayer graphene nanoribbons with armchair edges. *Applied Physics Letters*, *92*(22), 223106. https://doi.org/10.1063/1.2938058

Li, Z. Q., Henriksen, E. A., Jiang, Z., Hao, Z., Martin, M. C., Kim, P., Stormer, H. L., & Basov, D. N. (2009). Band structure asymmetry of bilayer graphene revealed by infrared spectroscopy. *Physical Review Letters*, *102*(3), 037403. https://doi.org /10.1103/PhysRevLett.102.037403

Loan, P. T. K., Zhang, W., Lin, C. T., Wei, K. H., Li, L. J., & Chen, C. H. (2014). Graphene/MoS_2 heterostructures for ultrasensitive detection of DNA hybridisation. *Advanced Materials*, *26*(28), 4838-4844. https://doi.org/10.1002/ adma.201401084

Lu, C. L., Chang, C. P., Huang, Y. C., Chen, R. B., & Lin, M. L. (2006). Influence of an electric field on the optical properties of few-layer graphene with AB stacking. *Physical Review B*, *73*(14), 144427. https://doi.org/10.1103/PhysRevB.73.144427

Mak, K. F., Lui, C. H., Shan, J., & Heinz, T. F. (2009). Observation of an electric-field-induced band gap in bilayer graphene by infrared spectroscopy. *Physical Review Letters*, *102*(25), 256405. https://doi.org/10.1103/PhysRevLett.102.256405

Malard, L. M., Elias, D. C., Alves, E. S., & Pimenta, M. A. (2008). Observation of distinct electron-phonon couplings in gated bilayer graphene. *Physical Review Letters*, *101*(25), 257401. https://doi.org/10.1103/PhysRevLett.101.257401

McCann, E. (2006). Asymmetry gap in the electronic band structure of bilayer graphene. *Physical Review B*, *74*(16), 161403. https://doi.org/10.1103/PhysRevB.74.161403

McCann, E., & Koshino, M. (2013). The electronic properties of bilayer graphene. *Reports on Progress in Physics*, *76*(5), 056503. https://doi.org/10.1088/0034-4885/76/5/056503

Min, H., Sahu, B., Banerjee, S. K., & MacDonald, A. H. (2007). *Ab initio* theory of gate induced gaps in graphene bilayers. *Physical Review B*, *75*(15), 155115. https://doi.org/10.1103/PhysRevB.75.155115

Nanda, B. R. K., & Satpathy, S. (2009). Strain and electric field modulation of the electronic structure of bilayer graphene. *Physical Review B*, *80*, 165430. https://doi.org/10.1103/PhysRevB.80.165430

Neto, A. H. C., Guinea, F., Peres, N. M. R., Novoselov, K. S., & Geim, A. K. (2009). The electronic properties of graphene. *Reviews of Modern Physics*, *81*(1), 109. https://doi.org/10.1103/RevModPhys.81.109

Novoselov, K. S., Fal'ko, V. I., Colombo, L., Gellert, P. R., Schwab, M. G., & Kim, K. (2012). A roadmap for graphene. *Nature*, *490*(7419), 192-200. https://doi.org/10. 1038/nature11458

Ohta, T., Bostwick, A., Seyller, T., Horn, K., & Rotenberg, E. (2006). Controlling the electronic structure of bilayer graphene. *Science*, *313*(5789), 951-954. https://doi.org/10.1126/science.1130681

Ruseckas, J., Juzeliūnas, G., & Zozoulenko, I. V. (2011). Spectrum of π electrons in bilayer graphene nanoribbons and nanotubes: An analytical approach. *Physical Review B, 83*(3), 035403. https://doi.org/10.1103/PhysRevB.83.035403

Sahu, B., Min, H., & Banerjee, S. K. (2010). Effects of magnetism and electric field on the energy gap of bilayer graphene nanoflakes. *Physical Review B, 81*(4), 045414. https://doi.org/10.1103/PhysRevB.81.045414

Scholz, A., Stauber, T., & Schliemann, J. (2012). Dielectric function, screening, and plasmons of graphene in the presence of spin-orbit interactions. *Physical Review B, 86*(19), 195424. https://doi.org/10.1103/PhysRevB.86.195424

Son, Y. W., Cohen, M. L., & Louie, S. G. (2006). Energy gaps in graphene nanoribbons. *Physical Review Letters, 97*(21), 216803. https://doi.org/10.1103/PhysRevLett.97.216803

Sun, S. J., & Chang, C. P. (2008). Ballistic transport in bilayer nano-graphite ribbons under gate and magnetic fields. *The European Physical Journal B, 64*, 249-255. https://doi.org/10.1140/epjb/e2008-00309-4

Vũ, T. T., Nguyễn, T. K. Q., Huỳnh, A. H., Phan, T. K. L., & Trần, V. T. (2017). Modulation of bandgap in bilayer armchair graphene ribbons by tuning vertical and transverse electric fields. *Superlattices and Microstructures, 102*, 451-458. https://doi.org/10.1016/j.spmi.2016.12.031

Vũ, T. T., Nguyễn, T. K. Q., Nguyễn, T. M. T., Nguyễn, V. C., & Trần, V. T. (2018). Enhancement of the Seebeck effect in bilayer armchair graphene nanoribbons by tuning the electric fields. *Superlattices and Microstructures, 113*, 616-622. https://doi.org/10.1016/j.spmi.2017.11.042

Vũ, T. T., & Trần, V. T. (2016). Electric gating induced bandgaps and enhanced Seebeck effect in zigzag bilayer graphene ribbons. *Semiconductor Science and Technology, 31*(8), 085002. https://doi.org/10.1088/0268-1242/31/8/085002

Xu, H., Heinzel, T., & Zozoulenko, I. V. (2009). Edge disorder and localization regimes in bilayer graphene nanoribbons. *Physical Review B, 80*(4), 045308. https://doi.org/10.1103/PhysRevB.80.045308

Zhang, Y., Tang, T. T., Girit, C., Hao, Z., Martin, M. C., Zettl, A., Crommie, M. F., Shen, Y. R., & Wang, F. (2009). Direct observation of a widely tunable bandgap in bilayer graphene. *Nature, 459*(7248), 820-823. https://doi.org/10.1038/nature08105

Zhong, X., Pandey, R., & Karna, S. P. (2012). Stacking dependent electronic structure and transport in bilayer graphene nanoribbons. *Carbon, 50*(3), 784-790. https://doi.org/10.1016/j.carbon.2011.09.033